national accelerator laboratory

TM-292
1101.200
1101.300

CALCULATION OF THE RADIONUCLIDE PRODUCTION IN THE SURROUNDINGS OF THE NAL NEUTRINO LABORATORY

M. Awschalom

March 11, 1971

ABSTRACT

For the design of beam dumps, target stations, and the Neutrino-Laboratory decay tunnel, it was necessary to gather previously unavailable data, to calculate the maximum amount of leachable radioactivity that may be produced annually in the surrounding soil, and to estimate that fraction of the radioactivity which may leave the site via the underground waters. This paper describes the calculations.

The Neutrino-Laboratory decay tunnel is discussed as an example. Making very conservative assumptions about underground water velocities, large average proton-beam currents (10^{13} p/sec, at 400 GeV, 100% of the time) and broad band neutrino beam operation (maximum beam power into the soil), it is shown that rather small amounts of H^3 (55 mCi/yr) and Na^{22} (31 μCi/yr) may leave the site.

The NAL accelerator will have more than one order of magnitude greater beam power than any other proton accelerator now in operation. Hence, it was necessary to study with some care the problem of soil radioactivation when high-energy protons interact with accelerator components and the secondary hadrons continue the development of the extranuclear cascade in the accelerator itself, enclosure, and surrounding soil. The concern with the radioactivation of the soil arises from the fact that some of the radioactivity so created may be leached away by the underground waters and be carried to off-site domestic water systems.

The problem may be divided into several parts:

1. The extranuclear cascade, activation, and spatial distribution of radionuclides;

2. Leachability of radionuclides from NAL soils;

3. Calculation of the leachable and non-leachable radioactivity created annually in the NAL soils; and

4. Transport of the radionuclides by the underground waters to the site boundaries.

Once the radioactivity leaving the site is estimated, it can be compared with the pertinent rules and regulations.[1]

In the treatment that follows, different approaches for solving a problem are discussed when possible. This makes the presentation

longer, but it may give a better feeling for the uncertainties involved in these calculations.

1. The Extranuclear Cascade

There is some uncertainty in the extranuclear cascade calculations because the most important input data, the source term, will only be known after the accelerator has become operational.

When a high-energy hadron undergoes a nonelastic event with a nucleus of the medium under consideration, it is said that a "star" has been created even if there is only one outgoing hadron. In the case of incident hadrons with energies of tens of GeV or greater, about 1 to 4 stars are produced per incident GeV of hadron kinetic energy.[2-4]

For any calculations involving stars and activations, nonelastic cross sections as well as activation cross sections are needed. The nonelastic cross sections of Belletini[5] are used, and they are assumed to be energy independent from about 30 MeV to the highest energy considered. For the sodium-22 activation, the cross-section calculations of Van Ginneken[6] are used. They are in excellent agreement with experimental results.[7-8] For the H-3 activation, experimental results are used exclusively.[7]

While studying the extranuclear cascade, we shall be interested in two of its characteristics:

1. The total number of radionuclides of a given type that are created per incident proton;

2. The spatial distribution of these radionuclides.

To calculate the quantity of nuclides and their distribution, two different but consistent approaches will be discussed below. They are:

(a) Some experimental results and Monte Carlo calculations

(b) Some other experimental results plus physical arguments.

a. The Monte Carlo Calculation

The calculation consists in picking random numbers to select polar and azimuthal angles as well as track lengths for the various hadrons produced in a collision, using energy-dependent mean free paths. Hadron momenta are chosen using random numbers and either Trilling's formula [9] for pions and or a modification of it for protons and neutrons. Energy is conserved at each interaction. Inelasticities are taken from cosmic-ray data when available and from R. G. Alsmiller's calculations [10] otherwise.

As the extranuclear cascade develops in configuration space, the star density and the energy spectra of the various components (p, n, and $\pi^{\pm}$) vary as functions of r and z, where r and z are cylindrical coordinates, with the incident primary hadron moving along the z-axis and the target-dump starting at z = 0.

There are three large Monte-Carlo programs to calculate extranuclear cascades. The first one, TRANSK, written by J. Ranft, [11] was later modified and improved at NAL by Ranft and Borak. [9]

J. Ranft used this more modern version to write a new program called FLUTRA.[12]

There is presently at NAL a greatly improved version of FLUTRA that has great versatility and that can reproduce all published shielding experiments carried out at 28 GeV within factors of two to three[13] over a range of fluxes of 10^5:1.

Figures 1 and 2 show the geometries of the Brookhaven experiment.[14,15] FLUTRA has been very successful in reproducing these results, as may be seen in Figs. 3-5. Figure 3 shows the prediction of the results for the side-shielding experiment of Bennett et al.[15] and actual results. Figure 4 is a prediction of the $C^{12} \rightarrow C^{11}$ activation in the beam-dump experiment[14] and actual results. Figure 5 is a prediction of the $Al^{27} \rightarrow F^{18}$ activation in the same dump[13] and the actual results. We can see that at 28 GeV the calculations are quite good for their intended use.

A virtue of FLUTRA is its simplicity. A much more elegant and accurate but slower program for similar calculations has been developed by R. G. Alsmiller and his group[10] at ORNL. In Alsmiller's model, the source function, i.e., the yield term, is the "extrapolation model,"[16] which is based on Bertini's nuclear model[17] for intranuclear cascades up to 3-GeV incident proton energy.[18] Figure 5 also shows Alsmiller's[19] prediction for the $Al^{27} \rightarrow F^{18}$ activation in the beam stop of the BNL experiment. This model makes more accurate predictions than

FLUTRA at 28 GeV. Other examples of this type of calculations may be found in Refs. 20 and 21.

Hence, we see that for energies up to 28 GeV, there are at least two independent programs that make absolute predictions very close to actual measurements. One should therefore consider their predictions for incident energies in the 200 to 500 GeV range to be probably as good as our ability to conceive source terms and so to predict particle production at higher energies. In particular, one should have additional confidence in Alsmiller's extrapolation model,[16] since it gives very good predictions of the π^- production at 75 GeV.

In practice, it is very difficult to separate the different components of the cascade in the midst of a thick shield. This is a consequence of the use of activation detectors for flux integration. Hence, it is customary to add all the components of the cascade into an undifferentiated hadronic flux. It is also customary to use the proton activation cross sections to estimate the magnitude of the undifferentiated hadron flux. Finally, it has also been customary to adopt an energy-independent value for the activation cross sections from threshold to maximum energy. Figure 6 shows, as an example, the C^{12} (n, 2n) C^{11} cross section as commonly used and the C^{12} (p, pn) C^{11} and C^{12} (p, pn)C^{11} as measured.[22] Figure 7 shows the measured Al^{27} (p, x) Na^{22} cross section as well as the macroscopic cross section for Na^{22}

activation in NAL soil. The present calculation, like many others,[6,23-25] recognizes that Na^{22} is produced by the spallation of Si, Fe, Ca, Mg, Na^{23}, K, etc.

In Table I, the macroscopic cross sections at 500 MeV for two types of NAL soils are presented. They show very similar nuclear characteristics in spite of their different natures. One is a composite of various NAL soils[26] and labeled "average NAL soil." The other one is from the glacial till at a location near the main accelerator.[7]

The results of the Monte-Carlo calculations may be used in various manners to calculate the production of a given nuclide.

For example, Armstrong[19,20,21,27] and Gabriel[20,27] use a complete intranuclear cascade at the site of a non-elastic event in order to determine the residual nucleus. In the NAL version of FLUTRA, the macroscopic activation cross section is entered as a dimensional array. In the program TRANSK the energy-dependent cross section is calculated using Rudstam's formula.[28]

In all cases, the quantity sought is

$$A_i = \int_V dV\, A_i(r,z) = \int_V dV \int_0^E \Sigma_i(E')\phi(E',r,z)\,dE', \qquad (1)$$

where $A_i(r,z)$ is the production of the i-th nuclide per incident hadron at a point (r,z) of the medium. Sometimes A_i is expressed in curies for a given incident current and energy and after a certain irradiation

Table I. ^{22}Na Macroscopic Cross Sections at E_h = 500 MeV
For NAL's Average Soils and Glacial Till.

		Average Soil						Glacial Till				
A	Element	% by Weight	N (a)	σ_{Na} (b)	$N\sigma_{Na}$ (c)	σ_{ne} (b)	$N\sigma_{ne}$ (c)	% by Weight dry	% by Weight moist	N (a)	$N\sigma_{Na}$ (b)	$N\sigma_{ne}$ (c)
16	O	55.0	2.07E22	0	0	0.31	0.642E22	50.8	56.5	2.13E22	0	0.660E22
28	Si	22.8	0.49	0.017	0.00833E22	0.47	0.230	25.7	21.8	0.47	0.0080E22	0.221
27	Al	5.51	0.123	0.013	0.00160	0.46	0.057	6.2	5.3	0.12	0.0016	0.0552
12	C	3.32	0.166	0	0	0.195	0.032	3.7	3.2	0.15	0	0.0292
1	H	1.23	0.737	0	0	0.025	0.018	-	1.67	1.01	0	0.0252
56	Fe	2.91	0.0314	0.0002	-	0.800	0.025	3.3	2.8	0.031	-	0.0248
40	Ca	6.08	0.0914	0.004	0.0037	0.62	0.057	6.8	5.8	0.087	0.00035	0.0539
25	Mg	2.09	0.0518	0.028	0.00145	0.43	0.022	2.4	2.0	0.050	0.0014	0.0215
23	Na	0.40	0.0104	0.036	0.00037	0.40	0.004	0.45	0.38	0.010	0.00036	0.0040
39	K	0.52	0.0080	0.004	0.00003	0.62	0.005	0.58	0.49	0.0077	0.00003	0.00471
				$\Sigma N_i \sigma_{i,Na}$ = 0.012E22						$\Sigma N_i \sigma_{i,Na}$ = 0.012E22		
						$\Sigma N_i \sigma_{i,ne}$ = 1.09E22						$\Sigma N_i \sigma_{i,ne}$ = 1.10E22

[a] atom/gram, moist soil
[b] barns
[c] barns/gram

time; E is the energy of the primary incident hadron, usually a proton; $\Sigma_i(E')$ is the macroscopic cross section for the formation of the i-th nuclide in the given medium by an undifferentiated hadron of energy E'; and $\phi(E',r,z)$ is the number of undifferentiated hadrons of energy E' per cm^2, per MeV per incident primary hadron, at a point (r,z) in the shield.

b. Experimental Results and Physical Arguments

The spatial distribution of the activity may be inferred from the measurements at CERN[29] and at BNL,[15] remembering that $p_\perp$ remains essentially unchanged as the energy of the incident hadron increases, while $p_{||}$ increases monotonically with $p_{incident}$.

T. Toohig[30] has estimated that about one-third of all the activity is created in the soil surrounding the decay pipe of the neutrino-beam facility and two-thirds is created in the beam stop at the end of the pipe. This fractionation is in good agreement with the Monte Carlo calculations of Gabriel.[27]

In order to calculate the number of atoms of some nuclide, some manipulation of the cross sections and assumptions regarding the energy spectrum of the hadrons must be made.

If the total number S of "stars" has been obtained by calculation or estimation from experimental results, the ratio A_i/S (nuclides of the i-th type to all stars) can be calculated from

$$\frac{A_i}{S} = \int_V dV \int_0^E \Sigma_i(x)\phi(x,r,z)\,dx \Big/ \int_V dV \int_0^E \Sigma(x)\phi(x,r,z)\,dx, \quad (2)$$

where $\Sigma(E)$ is the energy-dependent macroscopic nonelastic cross section for the given medium.

The distribution of the radionuclides is commonly assumed to be the same as that for all the stars, unless the activation cross section for the particular radionuclide is used as part of the calculation.

Certain simplifying assumptions are commonly made such as

1. A single energy spectrum is used throughout; then the flux term can be split into a product of an energy-dependent term and a spatially dependent term. That is,

$$\phi(E,r,z) \rightarrow N(E)\phi'(r,z). \quad (3)$$

This may underestimate the Na^{22} production by not more than 10-15% in some regions.

2. In such geometries as the Neutrino-Laboratory decay tunnel ϕ' is assumed to be independent of z, which is a good first approximation.[4,27] Using the activities at the maximum of the distribution, the total Na^{22} is overestimated by less than a factor of three.

The change of the constant-flux cardioids of revolution[4,14,31] into spheres makes no difference in practical applications such as target boxes, because the forward shielding is dictated by considerations other

than soil activities and usually is greater than that needed for soil protection.

Accepting the assumptions (a) and (b) above and that of energy-independent cross sections, then formula (1) becomes

$$A_i = \Sigma_i \int_V \phi(r,z)\, dV \int_{E_{th}}^{E} N(x)\, dx, \tag{4}$$

where E_{th} is the threshold energy for the macroscopic cross section Σ_i.

If a flux has been evaluated with a detector having a macroscopic cross section Σ_d and threshold energy $E_{th}(d)$, the two activities may be related by

$$A_i = A_d * (\Sigma_i/\Sigma_d) * \left[\int_{E_{th}(i)}^{E} N(x)\, dx \Big/ \int_{E_{th}(d)}^{E} N(x)\, dx \right] \tag{5}$$

where the subscripts i and d refer respectively to the nuclide under consideration and the monitoring detector used for flux evaluation in either a calculation or an experiment. Effectively, Eq. (5) is a re-written Eq. (1).

Figures 8 and 9 show graphs of the integral $\int_{E'}^{E} N(x)\, dx$ as a function of E' (the threshold energy) for incident protons of 200 and 500 GeV and soil as a moderating medium. They are taken from Ref. 8.

It is obvious that if a number S (total stars per incident hadron produced by hadrons with energy greater than a given threshold) is

known from some source, then the number of nuclides may be found by substituting A_d by S.

The number S may be calculated using the expression

$$S = kE_0, \tag{6}$$

where S is the total number of stars created in a given semi-infinite medium, by incident protons of kinetic energy E_0, by all secondaries with energy greater than or equal to E', and k is the proportionality constant that depends on the medium and E'.

The value of k may be obtained from experimental results by studying the activation of foils through beam stops or other geometries. The value of k given in Ref. 2 is of experimental origin. It is very comforting that the values of k agree so well.

For our calculations, we have adopted the value k = 4, because FLUTRA tends to underestimate the flux at large radii by a factor of approximately 3. Hence, k = 4 should be conservative.

Table II. Values of the Proportionality Constant k.

Medium	E'(MeV)	k	Source
steel	100	1.68	3
steel	15	4.36[a]	3
steel	47	0.8	4
soil	15	1.4	4
steel-soil	"?"	~1-2	2

[a] A proper fit in the 40 to 1000 GeV range requires $S = kE_0 + 75$

2. Measurements of the Macroscopic Cross Sections and Leachability of Various Radionuclides for NAL Soils

In order to calculate the production of radionuclides in the soil, one needs: (a) the distribution of the components of the hadronic cascade in the phase-space of the generalized target (dump, shield, etc.) and (b) the energy-dependent macroscopic cross sections for the production of the radionuclides of interest in the medium under consideration.

In Section 1 a discussion of methods for flux estimation were given. To obtain the activation macroscopic cross section for NAL soil, one may refer to published activation cross sections and calculate them. This is possible to do for Na^{22} and an example of such a calculation at one energy was given in Table I. In Ref. 6 the energy-dependent macroscopic cross section is calculated and plotted. Figure 9 is a reproduction of Fig. 7 of Ref. 6 of the macroscopic cross section versus energy.

From Table I, we get the ratio of the macroscopic cross section, $\Sigma(Na^{22})$ to Σ (nonelastic) to be approximately equal to 0.011.

A second method consists of taking samples of NAL soils and exposing them at the Argonne ZGS and Brookhaven AGS, near internal targets and behind one foot of concrete. The results of such measurements are given in Ref. 7.

The agreement between the measured macroscopic cross sections for Na^{22} and the calculated ones is excellent. From Ref. 7 we have

$$\Sigma_{meas}(Na^{22}) = 1.5 - 2.2\times10^{-4}\ cm^2g^{-1}$$

$$\Sigma_{calc}(Na^{22},\ 500\ MeV) = 1.2\times10^{-4}\ cm^2g^{-1}.$$

Note that the calculated Σ has a broad maximum at $1.7\times10^{-4}\ cm^2g^{-1}$.

A quantity that would be difficult to calculate is the fraction of the created activity of each radionuclide which would leach out in a first water pass and in subsequent water passes. Experimental results are given in Table III.

The importance of the fraction leached during subsequent washings of the soil is that it provides a means to calculate the relative ion velocity of the radionuclide in question with respect to the water velocity.

From the leachings following the first one, one can calculate the ion drift velocity using the expression[32]

$$Kd = \frac{q_A}{C_A} = \frac{(\mu Ci/g)\text{ in dry soil}}{(\mu Ci/ml)\text{ in solution}} = \left(\frac{ml}{g}\right), \qquad (7)$$

where Kd is the distribution coefficient, q_A is the radionuclide activity per gram of dry soil, and C_A is the radionuclide activity per ml of solution.

In actual practice, one can use the approximate relation

$$Kd = \frac{Co - C_E}{C_E} \times \frac{\text{volume of solution (ml)}}{\text{mass of dry soil (g)}}, \qquad (8)$$

where Co is the initial concentration of radioactivity (μCi/ml) in the solution, and C_E is the activity of the solution (μCi/g) after contact with the solution.

The diffusion coefficient Kd may then be used to calculate the relative velocity of the radionuclide with respect to the water carrying it.

$$\text{Relative velocity} = \frac{v(\text{radionuclide})}{v(H_2O)} = \frac{1}{1 + D}, \qquad (9)$$

where $D = Kd * (\rho_b / \epsilon)$ is a dimensionless quantity, ρ_b is the density of the dry soil (g/cm^3) and ϵ is the porosity (the fraction of the volume of dry soil occupied by the voids).

Formulas 7 and 9 were used in evaluating Kd for H^3 and Na^{22} in NAL's glacial fill. The results are given below:

Table III. Leachability of Sodium and Tritium.

Radionuclide	Na^{22}	H^3
Leachable Fraction, first wash	0.20	1.0
Leachable Fraction, other washes		
Kd	0.204	~0
Relative Velocity	0.44	1

The results of the batch work done at NAL are reported elsewhere.[7,33]

3. Calculation of Radionuclide Production

The beam parameters used in the calculations are

Table IV. Beam Parameters

Incident Proton Energy	= 400 GeV
Average Incident Proton Current	= 10^{13} protons/sec
Irradiation Time	>>half life of any one radionuclide under consideration.

All secondaries interact in the soil surrounding the point of interaction.

Note that the use of an average beam current implies some combination of actual beam current and duty cycle. In addition irradiation times much longer than the half-life of the radionuclide under consideration imply a condition of dynamic equilibrium between the number of radionuclides produced per second and the number of radionuclides decaying per second.

The calculations are summarized in Table V. Comparisons with calculations of other authors are also shown. The k's used are those of Table II, and for this work K = 4. The ratio of all Na^{22} stars to all stars is taken as 0.011, from Table I.

The activities derived from Ref. 27 were calculated averaging over all radii for the Z-interval 50 m to 100 m, and multiplying the activities is given by the ratio (400/500) to convert them to 400 GeV.

The calculations given below in Table V assume that all the beam power is dissipated in the soil. In Table VI, the geometry is taken into account.

The quantities given are total and leachable activity created per year. This rate of production is convenient for the calculation of the yearly activity leaving the site.

Table V. Comparison of Various Calculations for Yearly Radioactivity Production and Leaching from NAL Soils by a Proton Current of 10^{13} p/sec at 400 GeV.

Radionuclide	Radioactivity Production Rate(1) kCi/yr	Leachable Fraction	Leachable Radioactivity Production(1) kCi/yr	Reference
Na^{22}	3.04	0.20	0.608	2
Na^{22}	0.029	0.10	0.0029	30
Na^{22}	1.9	0.20	0.38	See a
Na^{22}	1.1	0.20	0.22	This work
Na^{22}	0.74	-	-	27
Na^{22}	0.41	-	-	34
H^{3}	0.34	-	-	27
H^{3}	1.1	1.0	1.1	This work
Ca^{45}	0.76	-	-	27
Ca^{45}	0.25	0.05-0.10	0.013	This work
Mn^{54}	0.40	-	-	27
Mn^{54}	0.054	0.003	-	This work

[a]The activity estimated in Ref. 30 was changed by the author of this note as follows:

1. Correction for Na^{22} macroscopic cross section. The macroscopic cross section given by Van Ginneken[6] at 100 MeV is used instead of only the aluminum spallation cross section. This gives an increase of 20 in the expected activity.
2. The energy scaling factor is taken as E^{+1}, instead of $E^{\frac{1}{2}}$, this gives an additional factor of $(400/30)^{\frac{1}{2}} = 3.65$.

3. The correction for threshold energy using the curves in Ref. 8, gives a factor of 0.90. Then, the activity created per year becomes

   activity/year (corrected) = 0.029 Ci/yr * 20 * 3.65 * 0.90

   = 1.9 k Ci/yr.

The Na^{22} activity created per year that has been estimated in this paper is just below the geometric mean of the maximum and minimum activities, $\sqrt{5 \times 7 * 0.41} = 1.5$ k Ci/yr.

To estimate the activity that may be leached annually to the aquifer, it is imperative to examine a drawing of the cross section of the neutrino laboratory meson decay pipe. This is shown in Fig. 10.

The cross-sectional area has been divided in sections for ease of calculations and for reasons of expected water flow. Sections 1 and 4 are backfilled with sand and gravel. Sections 3 and 3 are backfilled with compacted clay-like materials. Sections 5 and 6 are essentially undisturbed soils.

The significance of these sections is as follows. All radionuclides produced in Sections 1, 2, and 4 are assumed to be caught with 95% efficiency or greater by the imperious blanket.

Whatever escapes this "bathtub" is caught by the underdrains A and B. In addition, underdrains dry up a region determined, very approximately, by slopes of 5 in 1, near the tiles. These "draw-downs" form the lower boundaries of Section 5. It is also assumed

that the activity created in Sections 3 and 5 is collected. Then, only the activity created in Section 6 escapes to the aquifer.

To calculate the fraction of the stars created in each section, a radial dependence of the star density of the form

$$\phi(r) = \phi(r_0) r_0 \exp[-(r - r_0)\rho/\ell]/r, \qquad (7)$$

is assumed. Here, r_0 = 45 cm, ρ = 2.0 g/cm^3, and ℓ = 100 g/cm^2.

A cylindrical geometry is assumed and all matter is clay. Then, the relative fractions are given in Table VI.

Table VI. Distribution of Stars by Soil Section Perpendicular to Decay Pipe of Neutrino Laboratory.

Section	Fraction of All Stars
1	0.495
2	0.00402
3	0.000577
4	0.495
5	0.00500
6	1.14×10^{-4}

Now, we can calculate the maximum and minimum leachable radioactivity created in the vicinity of the decay pipe. Three sets of numbers will be calculated: maximum (Ref. 2), and minimum (Ref. 34).

Table VII. Annual Na^{22} Radioactivity Produced in the Soil.

	Minimum	This TM	Maximum	
Total	0.41	1.1	3.0	k Ci/yr
In Dump (2/3)	0.28	0.74	2.0	k Ci/yr
In Soil (1/3)	0.13	0.37	1.0	k Ci/yr
In zones 1, 2, and 4 (0.994)	0.13	0.37	1.0	k Ci/yr
In zones 3 and 5 (0.0056)	0.73	2.1	5.6	Ci/yr
In zone 6	0.015	0.042	0.11	Ci/yr
Leachable in zone 6	3.0	8.4	22.	m Ci/yr

Similar calculations may be carried out for H^3.

Table VIII. Annual H^3 Radioactivity Produced in the Soil.

	Minimum	This TM	Maximum	
Total	0.41	1.1	3.0	k Ci/yr
In Dump (2/3)	0.28	0.74	2.0	k Ci/yr
In Soil (1/3)	0.13	0.37	1.0	k Ci/yr
In zone 6	15	42	110	m Ci/yr
Leachable in zone 6	15	42	110	m Ci/yr

The concept of the gravel and the "bathtub" as well as that of the underdrains and creation of "draw-down" surfaces were discussed with representatives of the Illinois State Water Survey.[35] It was considered adequate by them.

4. Transport of Radionuclides.

We now have to estimate the travel time for the Na^{22} and H^3 from the vicinity of the decay pipe to the aquifer and along the aquifer to the site boundary.

The vertical velocity of the water in the glacial till is estimated to be 8 ft/yr,[36] and 3.6 to 7.2 ft/yr.[37] Here, a conservative value of

7.2 ft/yr will be used. Now the Na ion velocity[33] is about 0.44 that of water, because of ion-exchange processes taking place. Hence, the Na^{22} ion velocity is taken to be 3.2 ft/yr. For H^3, the ion velocity and the water velocity are the same.

It is now possible to estimate the transit times to the aquifer for Na^{22} and H^3:

Vertical distance ≃ 70 ft
Na^{22} transit time ≃ 70/3.2 = 21.9 years
H^3 transit time ≃ 70/7.2 = 9.72 years.

Since the respective half-lives are 2.6 and 12.3 years, the surviving fractions are

$$Na^{22} \text{ surviving fraction} = \exp(-21.9 \ln 2/2.6) = 2.91 \times 10^{-3}$$

$$H^3 \text{ surviving fraction} = \exp(-9.72 \ln 2/12.3) = 0.58.$$

The horizontal velocity of water in the aquifer is relatively large. Hence it is now assumed that all ions travel with the velocity of water.

The horizontal velocity is estimated at 3-6 ft/day, with a maximum of 13 ft/day.[36] The distance from the decay pipe to the site boundary in a southeasterly direction, as it is expected to flow from measured gradients,[37] is about 4 km. Then the horizontal transit time becomes,

$$T_h = 4 \times 10^3 \text{ m}/(13 \text{ ft/day} \times 365 \text{ day/year} \times 0.304 \text{ m/ft})$$
$$= 2.7 \text{ years}.$$

Surviving fractions,

$$Na^{22} \text{ fraction} = \exp(-2.7 \ln 2/2.6) = 0.49$$
$$H^{3} \text{ fraction} = \exp(-2.7 \ln 2/12.3) = 0.86.$$

Finally, it is possible to estimate the radioactivity reaching the aquifer and the site boundaries.

Table IX. Production of Annual Radioactivity Reaching the Aquifer.

	Na^{22}	H^{3}	
Leachable, zone 6	3.0-8.4-22.	15. -42. -110.	m Ci/yr
Reaching aquifer	0.0087-0.024-0.064	8.7-24. -64	m Ci/yr
Reaching site boundary	0.004-0.012-0.031	7.5-21. -55	m Ci/yr

5. Conclusions

The present estimates of the annual amounts of radioactivity leaving the site are quite conservative since they include the maximum reasonable ion velocity both vertically and horizontally.

In addition, the leachable fraction of the total activity was mesured by the batch process. This certainly gives an upper limit to the leachability.

Finally, both a high beam power and 100% duty cycle of the broad band neutrino facility have been assumed. This is certainly a gross overestimate. It is, therefore, felt that the estimates of the annual radioactivities leaving the site as given in Table IX are very cautious and conservative.

REFERENCES

[1] AEC Manual, Standards for Radiation Protection, Chapter 0524.

[2] R. H. Thomas, Possible Contamination of Ground Water System by High Energy Proton Accelerators, Lawrence Radiation Laboratory Report UCRL-20131, October, 1970.

[3] R. T. Santoro and T. A. Gabriel, to appear as an Oak Ridge National Laboratory Report.

[4] A. Van Ginneken, Hadron Shielding Calculations: Effects of Voids, National Accelerator Laboratory Internal Report TM-287, March 12, 1971.

[5] G. Belletini et al., Proton-Nuclei Cross Sections at 20 GeV, Nucl. Phys. 79 (609) 1966.

[6] A. Van Ginneken, Na^{22} Production Cross Section in Soil, National Accelerator Laboratory Internal Report TM-283, January 15, 1971.

[7] M. Awschalom et al., The Underground Water Leaching of Radionuclides. . ., to appear in IEEE Trans. Nucl. Sci, 1971.

[8] M. Awschalom, T. Borak, and H. Howe, Neutron Dosimetry: Expected Neutron Spectra. . ., National Accelerator Laboratory Internal Report TM-266, August 26, 1970.

[9] J. Ranft and T. Borak, Improved Nucleon-Meson Cascade Calculations, National Accelerator Laboratory Report FN-193, November 21, 1969.

[10] R. G. Alsmiller, private communications.

[11] J. Ranft, Improved Monte Carlo Calculation of the Nuclear-Meson Cascade in Shielding Materials, CERN-MPS/Int. MU/EP66-8, August 15, 1966.

[12] J. Ranft, private communication.

[13] A. Van Ginneken, M. Awschalom, and T. Borak, Beamstop Experiment at 29.4 GeV/c, Proc. 1971 Particle Accelerator Conference, Chicago, Illinois, March 1-3, 1971.

[14] G. W. Bennett et al., Study of a Uniform Steel Beam Stop at 28 GeV, Proc. 1971 Particle Accelerator Conference, Chicago, Illinois, March 1-3, 1971.

[15] G. W. Bennett et al., Flux Attenuation in a Steel Side Shield at the AGS, Proc. 1971 Particle Accelerator Conference, Chicago, Illinois, March 1-3, 1971.

[16] T. A. Gabriel, R. G. Alsmiller, and M. P. Guthrie, An Extrapolation Model for Predicting Nucleon and Pion Differential Production Cross Sections. . . , Oak Ridge National Laboratory Report ORNL-4542, May 1970.

[17] H. W. Bertini, Low Energy Intranuclear Cascade Calculation, Phys. Rev. 131, 1801 (1963) and correction in Phys. Rev. 138, 7AB, AB2 (June 28, 1965).

[18] H. W. Bertini, A. H. Culkowski, and M. P. Guthrie, Intranuclear Cascade Calculation of Secondary Nucleon Spectra. . . , Oak Ridge National Laboratory Report ORNL-TM-2361, March 14, 1969.

[19]T. W. Armstrong et al., Monte Carlo Calculations of High Energy Nucleon-Meson Cascades. . . , to be published.

[20]T. W. Armstrong and R. G. Alsmiller, Calculation of the Residual Photon Dose Rate Around High-Energy Proton Accelerators, Oak Ridge National Laboratory Report ORNL-TM-2498, February 10, 1969.

[21]T. W. Armstrong and J. Barish, Calculation of the Residual Photon Dose Rate Due to the Activation of Concrete. . . , Oak Ridge National Laboratory Report ORNL-TM-2630, June 23, 1969.

[22]St. Charalambus et al., Particle Flux Measurements with Activation Detectors, CERN/DI/HP90 (July 14, 1966).

[23]T. A. Gabriel, Calculation of the Long Lived Induced Activity in the Soil. . . , Oak Ridge National Laboratory Report ORNL-TM-3033, August 12, 1970.

[24]W. S. Gilbert et al., Concrete Activation Experiment at the Bevatron, Lawrence Radiation Laboratory Report UCRL-19368, December 18, 1969.

[25]P. J. Gollon et al., Experimental Results on High Energy Particle Production of Na^{24} in Concrete, National Accelerator Laboratory Internal Report TM-250, May 26, 1970.

[26]M. Awschalom, Chemical Composition of Some Common Shielding Materials, National Accelerator Laboratory Internal Report TM-168, May 2, 1969.

[27]T. A. Gabriel and R. T. Santoro, Calculation of the Long-Lived Activity in Soil Produced by 500-GeV Protons, Oak Ridge National Laboratory Report ORNL-3262, December 21, 1970.

[28]G. Rudstam, Systematics of Spallation Yields, Zeitsch. f. Naturforsch 21a, 1027 (1966).

[29]W. S. Gilbert et al., 1966 CERN-LRL-RHEL Shielding Experiment at the CERN Proton Synchrotron, Lawrence Radiation Laboratory Report UCRL-17941, September 1968.

[30]T. Toohig, A Calculation of the Na^{22} Produced in the Soil and in Ground Water. . . , National Accelerator Laboratory Internal Report TM-284, January 1971.

[31]A. R. Smith, Radiation Field Inside a Thick Concrete Shield. . . , Lawrence Radiation Laboratory Report UCRL-11331, September 18, 1964.

[32]L. H. Baetslé, Health Physics, Vol. 2, Part I, in A. M. F. Duhamel, (Pergamon Press, New York, 1969).

[33]T. Borak et al., The Underground Migration of Radionuclides. . . , to be published.

[34]A. Van Ginneken et al., Comparison of Measurements and Calculations for a 29.4 GeV/c steel Beam Stop, to appear in Proc. of the International Congress Protection Against Accelerator and Space Radiation, CERN, April 26-30, 1971.

[35]H. F. Smith, Illinois State Water Survey, private communication, January 19, 1971.

[36]T. Borak and P. J. Gollon, Some Geological and Hydrological Data at the NAL Site, National Accelerator Laboratory Internal Report TM-248, May 21, 1970.

[37]H. F. Smith, private communication.

FIGURE CAPTIONS

Fig. 1. Geometry of the beam-stop equipment. The steel and air gap width, used in the calculations, are given.

Fig. 2. Geometry of the side shield experiment.

Fig. 3. Comparison of predictions[34] and measurements[15] in the BNL side shield experiment.

Fig. 4. Comparison of carbon activation results[14] and predictions[34] in the BNL beam-stop experiment.

Fig. 5. Comparison of the Al^{27} (hadron ?) F^{18} results[13] and predictions by the NAL group[34] as well as those of Alsmiller's.[10]

Fig. 6. The C^{12} (p, pn) C^{11} and C^{12} (n, Zn) C^{11} measured cross sections[22] (solid lines) and its energy-independent approximation[29] (dashed lines).

Fig. 7. The Al^{27} (p, x) Na^{22} measured cross section[22] as well as the macroscopic activation cross section for Na^{22} in NAL soil.[6]

Fig. 8. Graph of the function $\phi(E') = \int_{E'}^{E} N(x)\,dx$ where E' = threshold energy and N(x) is the undifferentiated hadron flux. Case: lateral shielding of 200-GeV protons lost on steel (200 g/cm^2) and soil to a total thickness of 1500 g/cm^2.[29]

Fig. 9. Same as Fig. 8, but for 500 GeV protons and secondaries. Data from spectrum given in Ref. 27.

Fig. 10. Cross section through the decay pipe of the neutrino laboratory showing the different types of fill and the undisturb soils.

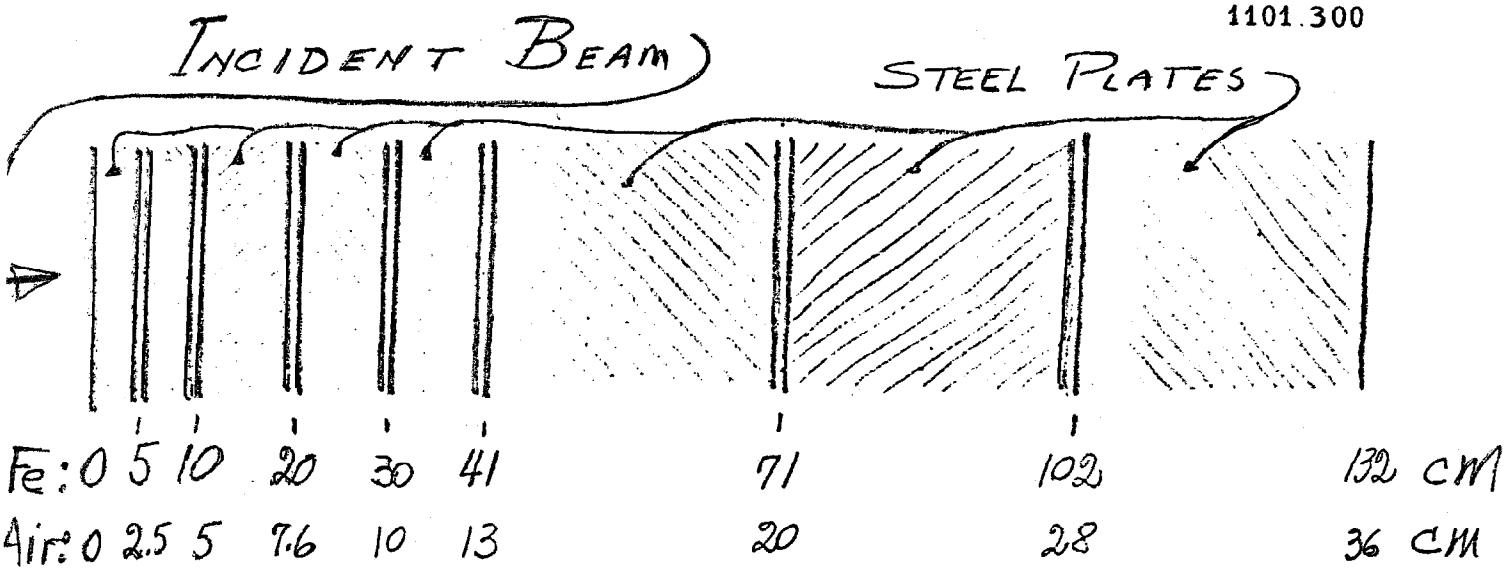
INCIDENT BEAM
STEEL PLATES
Fe: 0 5 10 20 30 41 71 102 132 cm
Air: 0 2.5 5 7.6 10 13 20 28 36 cm

Fig. 1

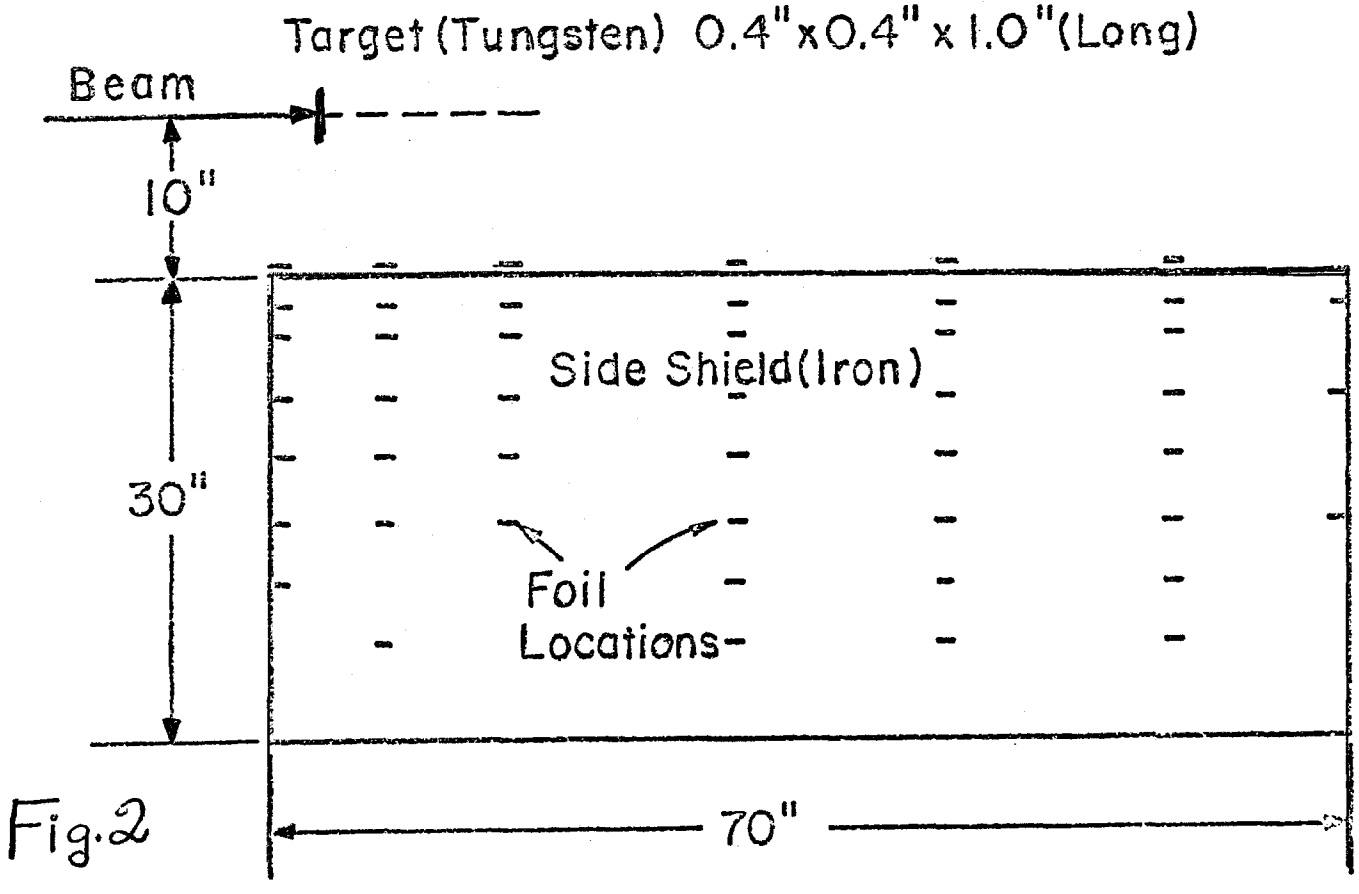
Target (Tungsten) 0.4"x0.4"x1.0"(Long)
Beam
10"
Side Shield(Iron)
30"
Foil
Locations
70"

Fig. 2

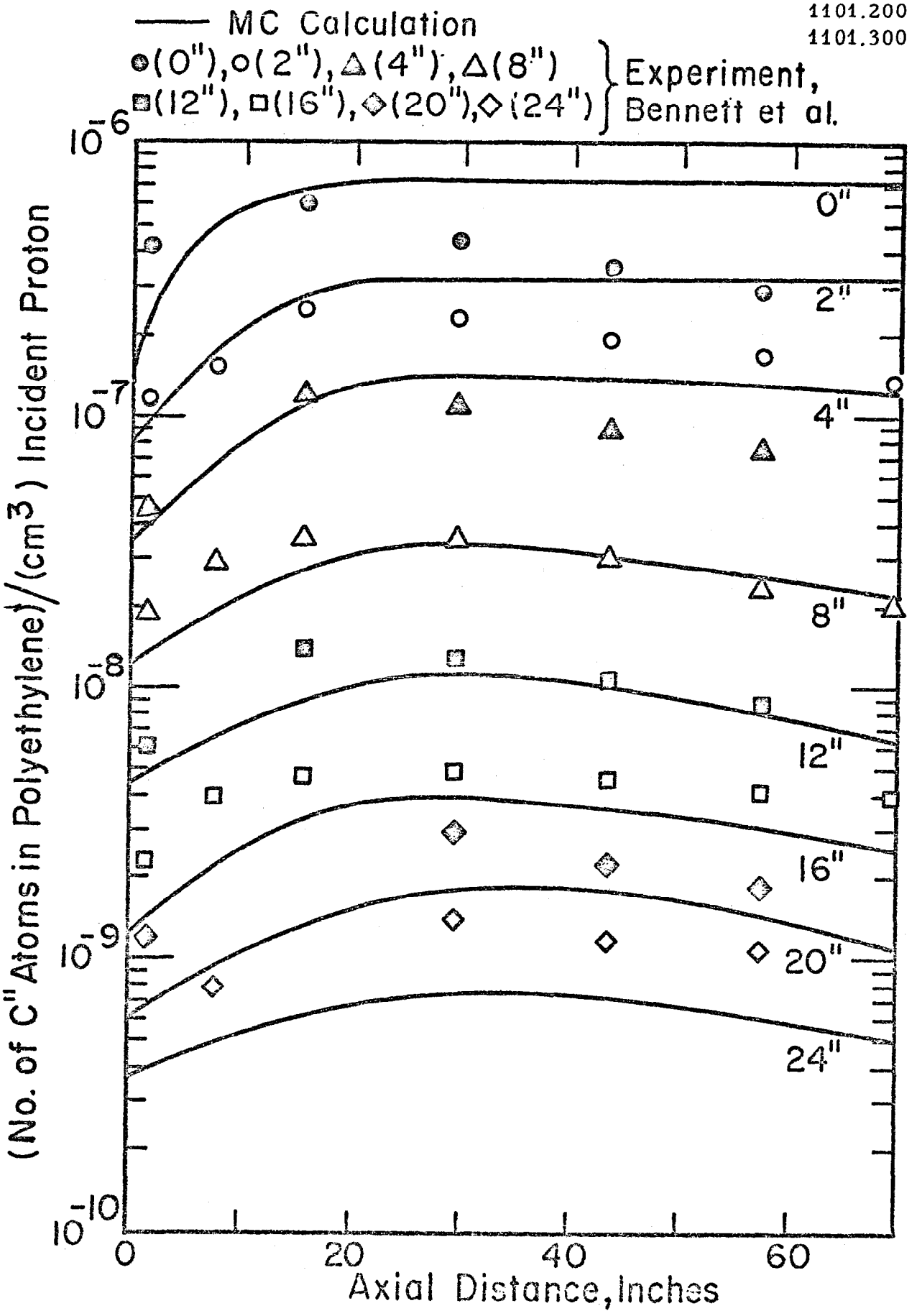
MC Calculation
●(0"),○(2"),△(4"),△(8")
■(12"),□(16"),◇(20"),◇(24")
Experiment, Bennett et al.
(No. of C" Atoms in Polyethylene†)/(cm³) Incident Proton
10⁻⁶
10⁻⁷
10⁻⁸
10⁻⁹
10⁻¹⁰
0"
2"
4"
8"
12"
16"
20"
24"
0
20
40
60
Axial Distance, Inches

Fig. 3

Fig. 4

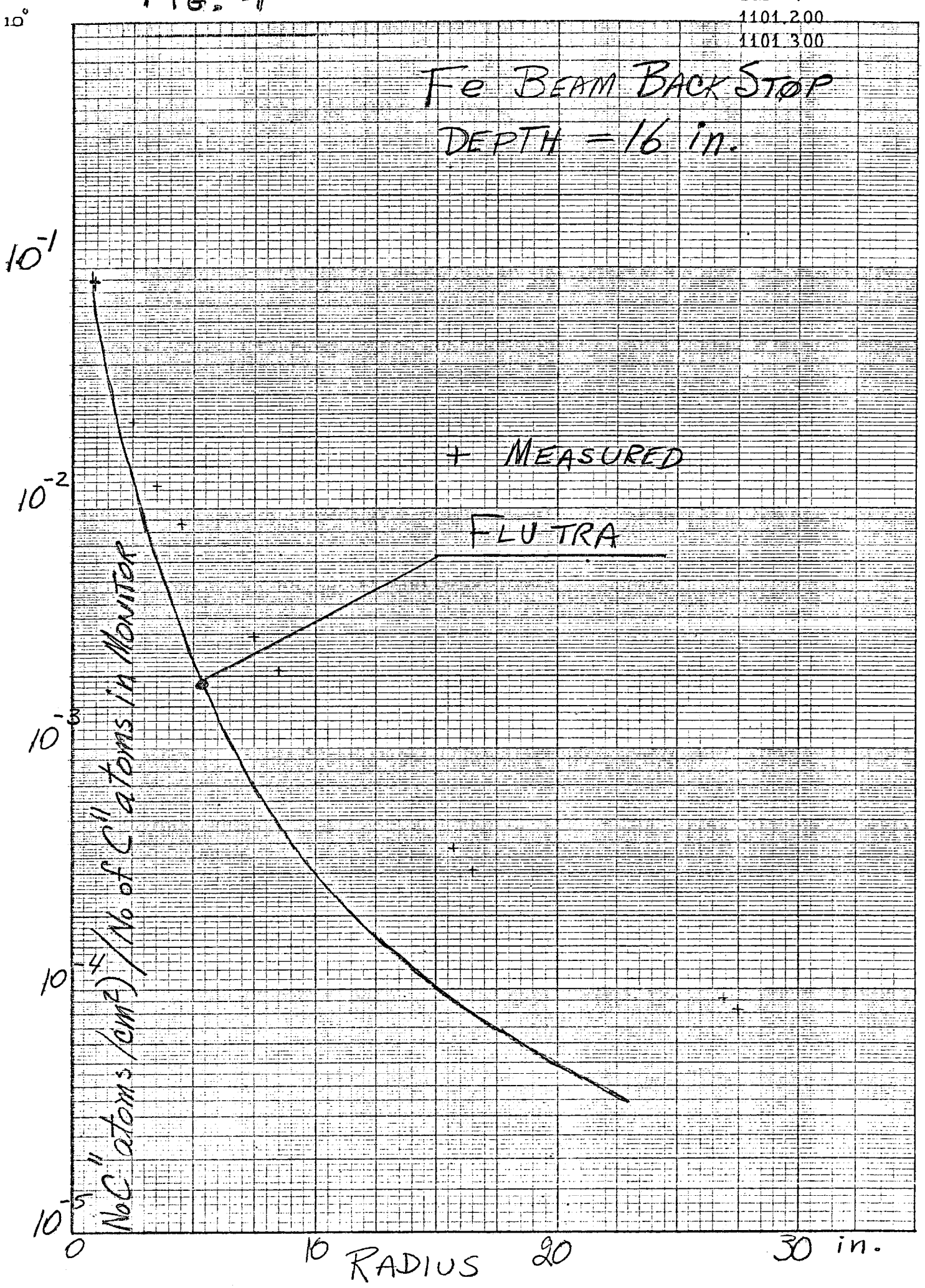
Fe BEAM BACK STOP
DEPTH = 16 in.
+ MEASURED
FLUTRA
No. Cl atoms/(cm²)/No. of Cl atoms in Monitor
10°
10⁻¹
10⁻²
10⁻³
10⁻⁴
10⁻⁵
0
10
20
30 in.
RADIUS

Fig. 5

1101.200
1101.300

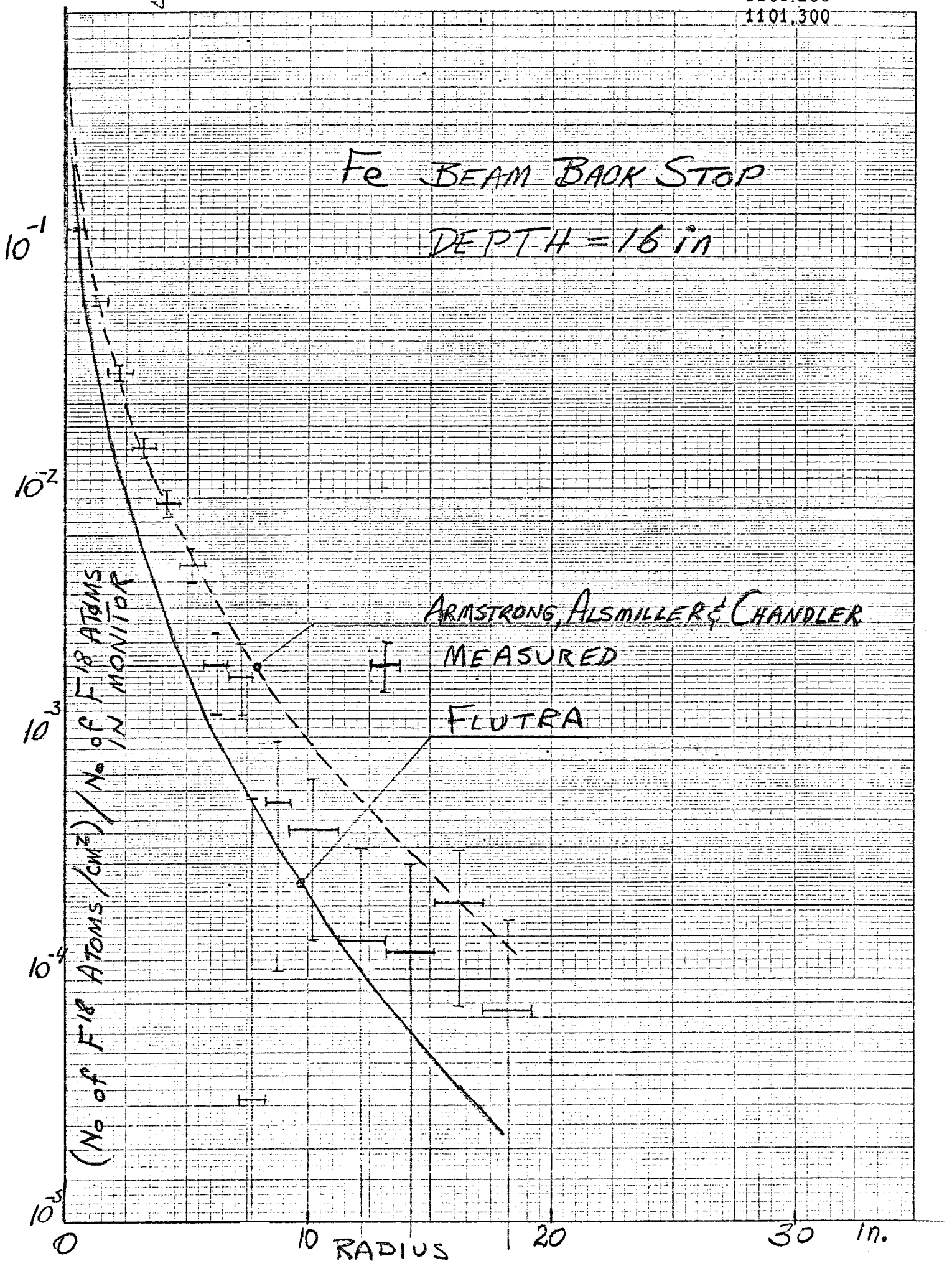

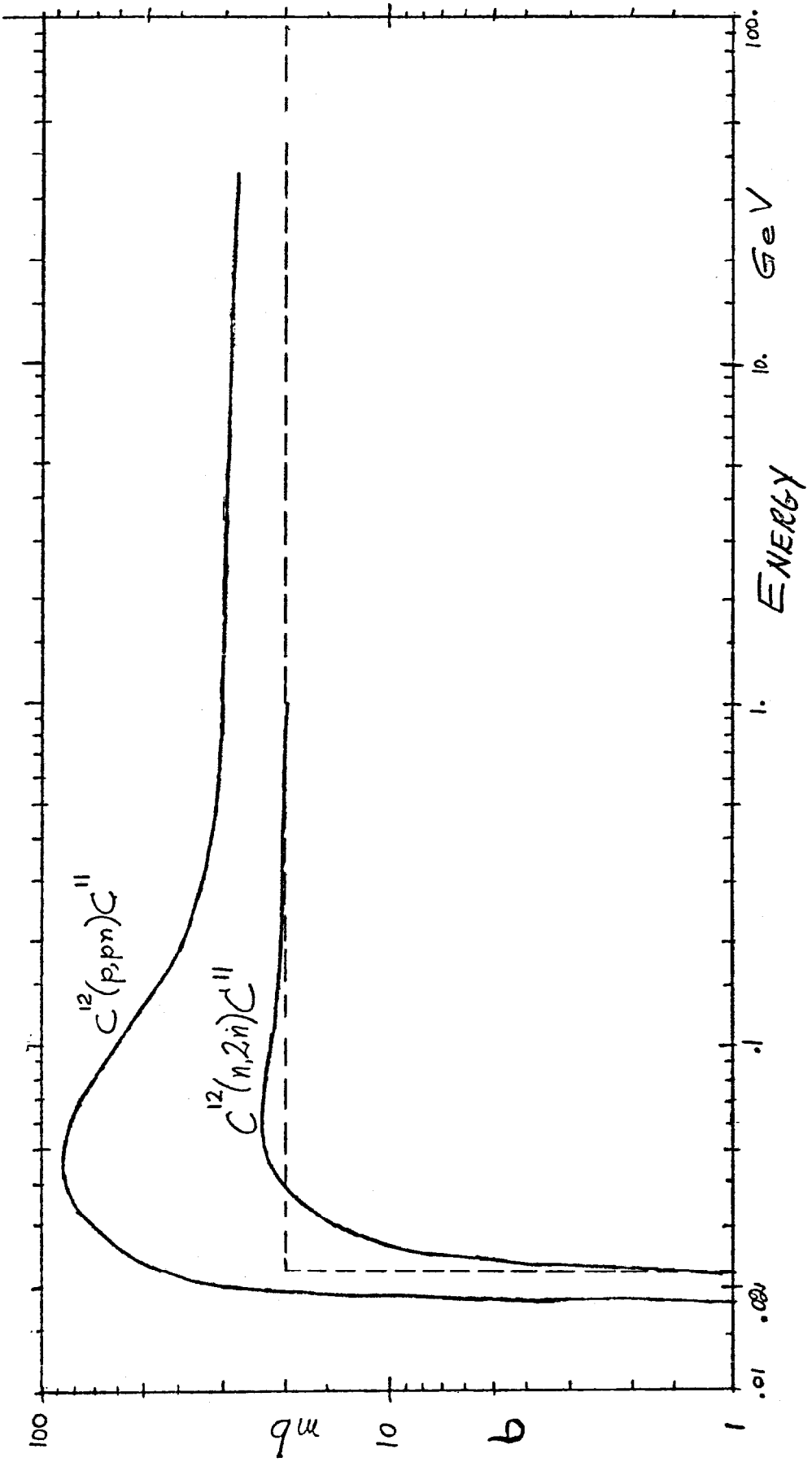

Fig 6

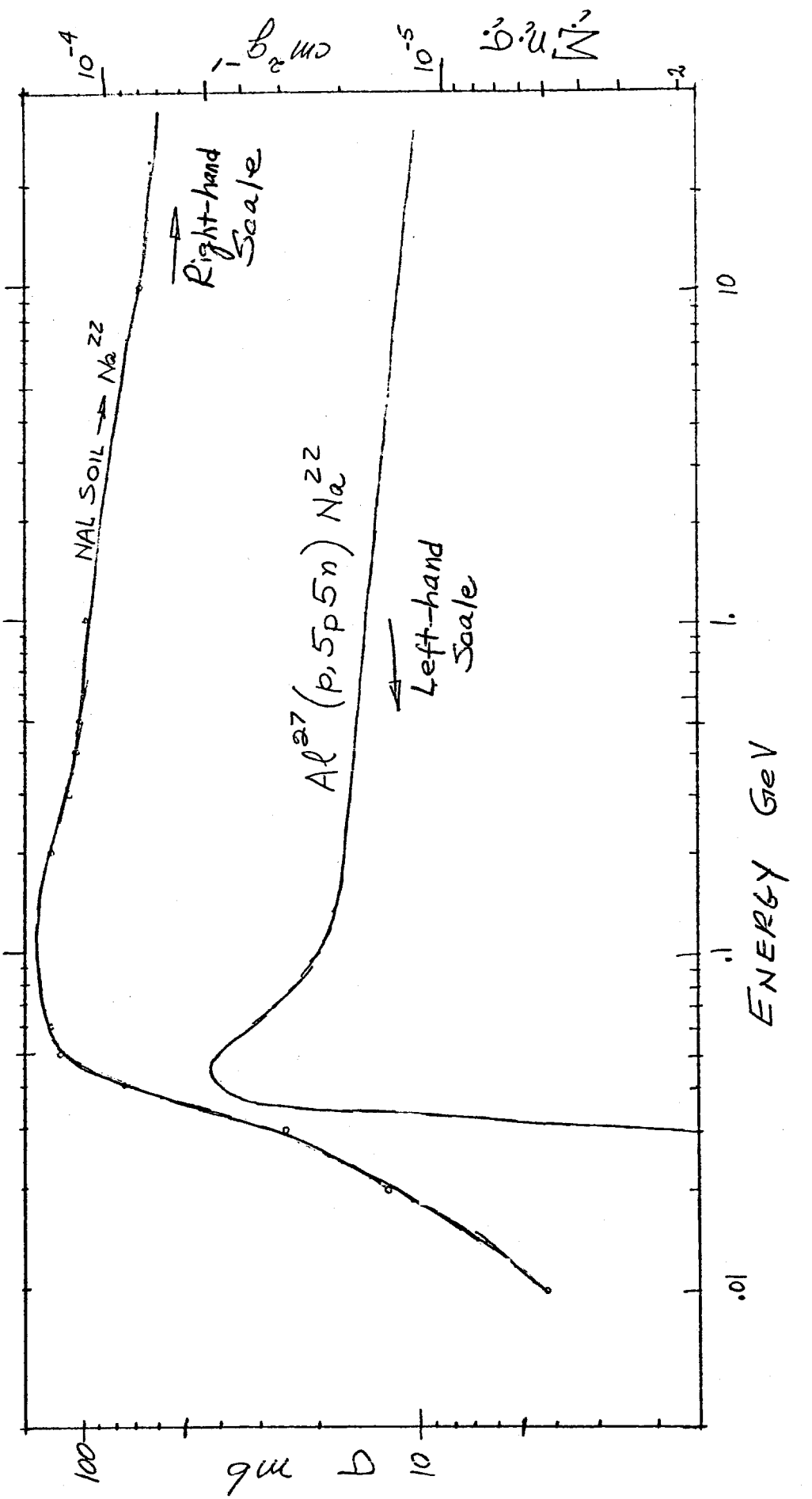
10^{-4}
cm^2 - b_z
10^{-5}
$\Sigma n_i \cdot \rho_i$
2
NAL Soil → Na^{22}
Right-hand Scale
$Al^{27}(p,5pn)Na^{22}$
Left-hand Scale
10
1.
.1
.01
ENERGY GeV
100
mb
10
σ

Fig 7

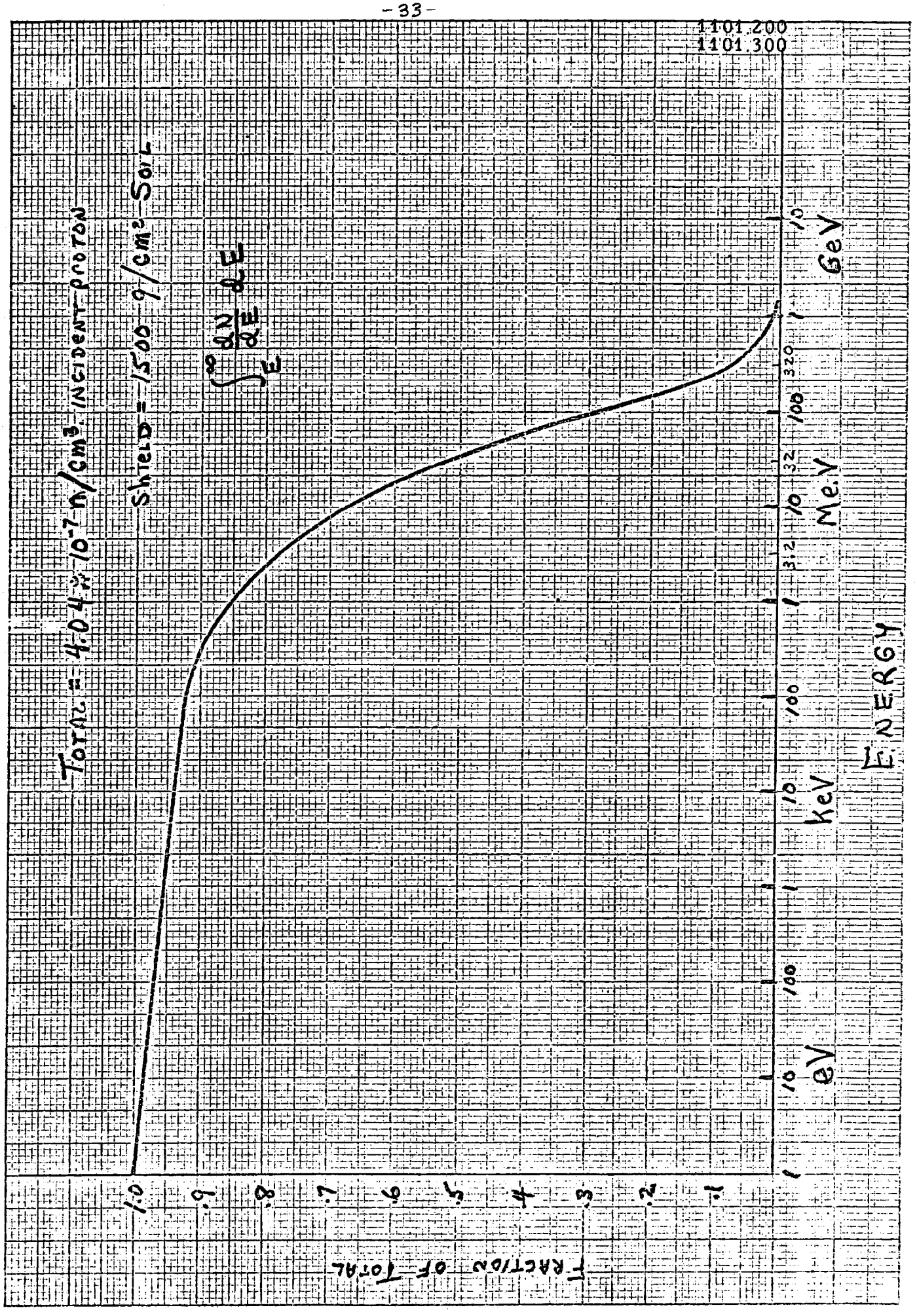
1101.200
1101.300
TOTAL = 4.04 × 10⁻⁷ n/cm³-INCIDENT-PROTON
SHIELD = 1500 g/cm²-Soil
∫ (dN/dE) dE
FRACTION OF TOTAL
1.0
.9
.8
.7
.6
.5
.4
.3
.2
.1
1
10
100
1
10
100
1
3.2
10
32
100
320
1
10
eV
keV
MeV
GeV
ENERGY

Fig. 8

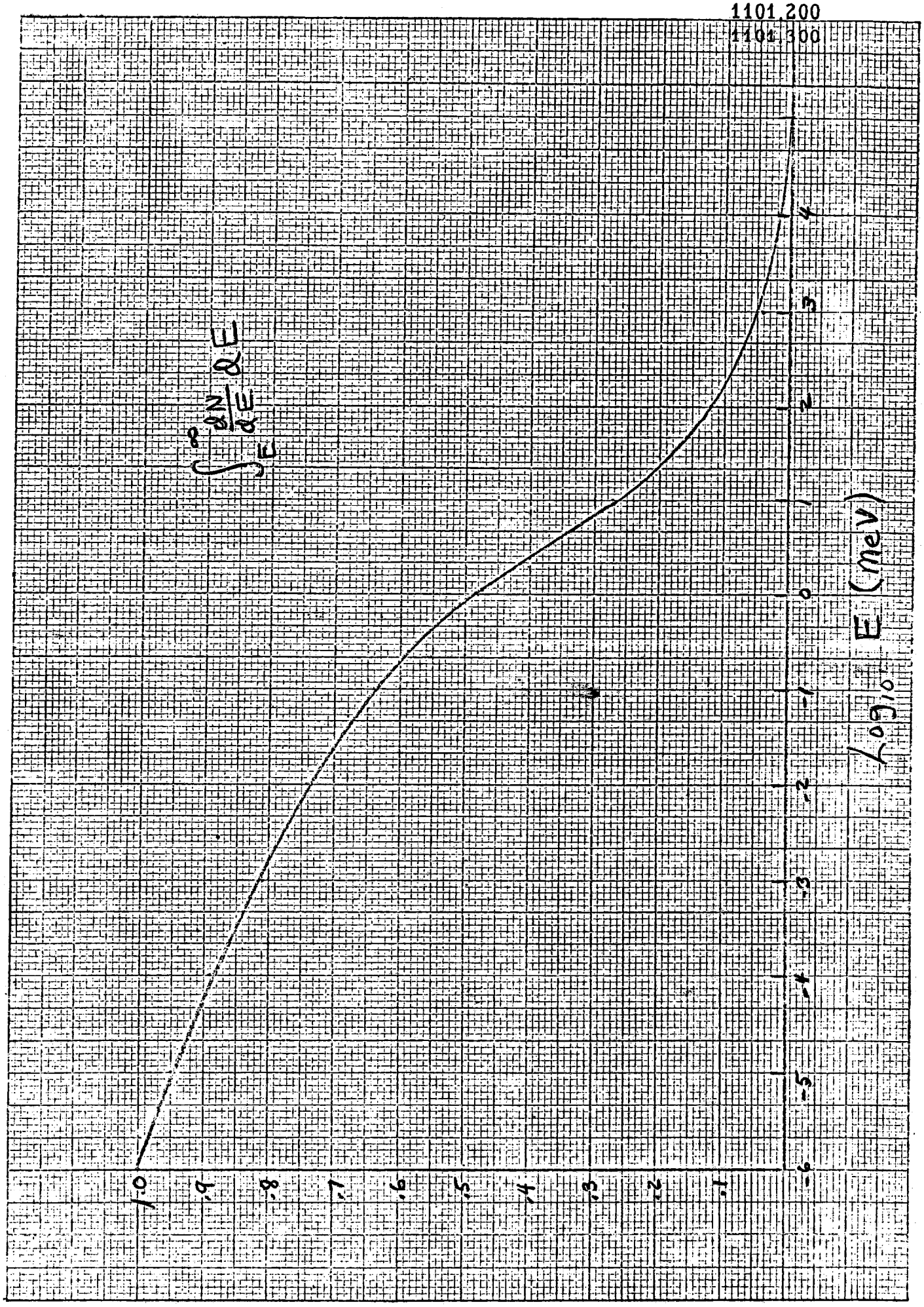
$\frac{1}{E}\frac{dN}{dE}$
$\log_{10}$ E (meV)
0.1
0.2
0.3
0.4
0.5
0.6
0.7
0.8
0.9
1.
2.
3.
4.
5.
6.
7.
8.
9.
-3
-2
-1
0
1
2
3
4

Fig. 9

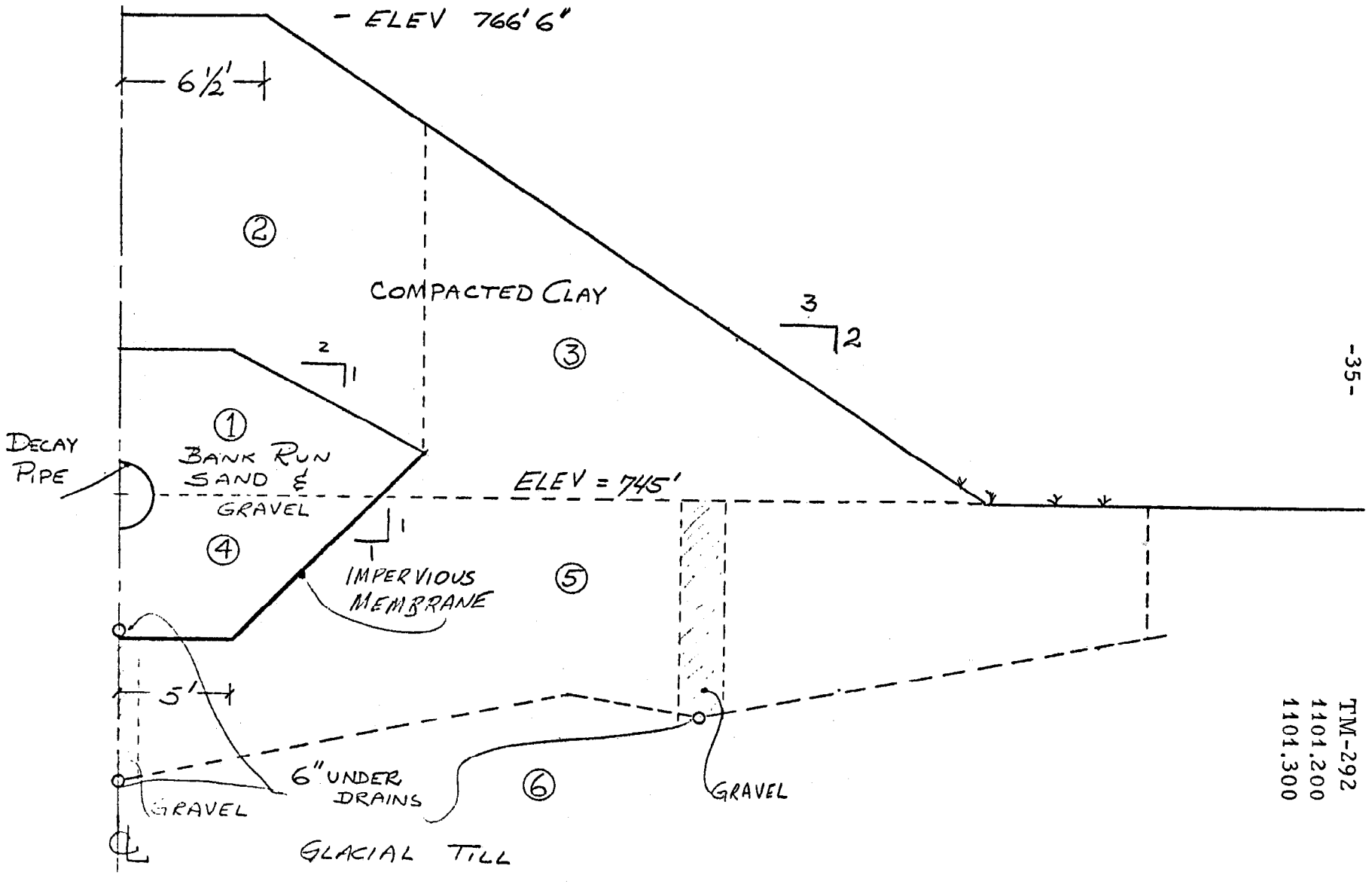

Fig 10

TM-292
1101.200
1101.300